

Modelling the impact of climate change on sediment yield in a highly erodible Mediterranean catchment

Gianbattista Bussi · Félix Francés · Enguerrand Horel · José Andrés López-Tarazón · Ramón J. Batalla

Received: 13 September 2013 / Accepted: 30 July 2014 / Published online: 16 August 2014
© Springer-Verlag Berlin Heidelberg 2014

Abstract

Purpose The assessment of climate change impacts on the sediment cycle is currently a primary concern for environmental policy analysts in Mediterranean areas. Nevertheless, quantitative assessment of climate change impacts is still a complex task. The aim of this study was to implement a sediment model by taking advantage of sediment proxy information provided by reservoir bottom deposits and to use it for climate change assessment in a Mediterranean catchment.

Materials and methods The sediment model was utilised in a catchment that drains into a large reservoir. The depositional history of the reservoir was reconstructed and used for

sediment sub-model implementation. The model results were compared with gauged suspended sediment data in order to verify model robustness. Then, the model was coupled with future precipitation and temperature scenarios obtained from climate models. Climatological model outputs for two emission scenarios (A2 and B2) were simulated and the results compared with a reference scenario.

Results and discussion Model results showed a general decrease in soil moisture and water discharge. Large floods, which are responsible for the majority of sediment mobilisation, also showed a general decrease. Sediment yield showed a clear reduction under the A2 scenario but increased under the B2 scenario. The computed specific sediment yield for the control period was $6.33 \text{ Mg ha}^{-1} \text{ year}^{-1}$, while for the A2 and B2 scenarios, it was 3.62 and $7.04 \text{ Mg ha}^{-1} \text{ year}^{-1}$, respectively. Furthermore, sediment transport showed an increase in its time compression, i.e. a stronger dependence of total sediment yield from the largest event contributions.

Conclusions This study shows a methodology for implementing a distributed sediment model by exploiting reservoir sedimentation volumes. This methodology can be applied to a wide range of catchments, given the high availability of reservoir sedimentation data. Moreover, this study showed how such a model can be used in the framework of a climate change study, providing a measure of the impact of climate change on soil erosion and sediment yields.

Keywords Climate change · Ésera River catchment · Reservoir sedimentation · Sediment modelling · TETIS

Responsible editor: José Carlos de Araújo

G. Bussi · F. Francés · E. Horel
Research Institute of Water and Environmental Engineering,
Universitat Politècnica de València, Camino de Vera s/n,
46022 Valencia, Spain

E. Horel
École des Ponts Paris Tech, Marne-la-Vallée, France

J. A. López-Tarazón
School of Natural Sciences and Psychology, Liverpool John Moores
University, Liverpool, UK

J. A. López-Tarazón · R. J. Batalla
RIUS, Fluvial Dynamics Research Group, Department of
Environment and Soil Sciences, University of Lleida, Lleida, Spain

R. J. Batalla
Catalan Institute for Water Research, Girona, Spain

R. J. Batalla
Forest Science Centre of Catalonia, Solsona, Spain

G. Bussi (✉)
School of Geography and the Environment, University of Oxford,
South Parks Road, OX13QY Oxford, UK
e-mail: gianbattista.bussi@ouce.ox.ac.uk

1 Introduction

At the present time, one of the main concerns of soil erosion research throughout the world is the assessment of climate change impact on the sediment cycle (Mullan et al. 2012). The

increase of global temperature is expected to affect the extent, frequency and magnitude of soil erosion and sediment redistribution (Peizhen et al. 2001; Pruski and Nearing 2002). This will probably lead to a more vigorous hydrological cycle (Nearing et al. 2005) and to the increased erosive power of rainfall (Nearing et al. 2004). Nevertheless, contrasting impacts were recently noticed in differing regions of the world. For example, Zhao et al. (2013) observed not only a strong increase in sediment export from the Loess Plateau of China due to anthropogenic causes but also detected significant reduction in both stream flow and sediment load along with recent climatic change. Foster et al. (2012) analysed changes in sediment transport for the Karoo uplands (South Africa). They observed a generalised increase in sediment yield rates during past decades, linked to an increase in the frequency of high magnitude rainfall events, among other factors.

Expected effects of climate change on soil erosion can be classified into on-site and off-site effects (Mullan et al. 2012). On-site effects are, for example, soil loss and decrease in soil productivity and will especially affect highly erodible areas such as tropical and sub-tropical ecosystems. Among off-site effects, muddy flows, reservoir sedimentation and water pollution can be cited.

These issues are of particular importance for Mediterranean areas, due to the high sensitivity of Mediterranean environments to both natural and human-induced alteration. Various studies have reported a general decrease in total precipitation and runoff (e.g. Milly et al. 2005) along with an increase in extreme rainfall (e.g. Alpert et al. 2002). However, only a few papers have assessed and quantified the impact of climate change on soil erosion and sediment transport in Mediterranean catchments. For example, Lavee et al. (1998) analysed the evolution of land cover and soil erosion of a Mediterranean transect under changing climatological conditions, while Cerdà (1998) demonstrated that the appearance of overland flow (and soil erosion as a consequence) can be triggered by a reduction in mean annual rainfall. Due to the extreme relevance of climate-induced soil erosion changes, their assessment and prediction are especially important.

The most common way to evaluate and quantify climate change impact on soil erosion and sediment transport is through a mathematical modelling approach. Sediment models are fundamental tools for soil erosion and sediment yield estimation. In particular, distributed modelling can provide important information about sediment redistribution, erosion and deposition zones and land use change effects (Van Rompaey et al. 2001). During the last 15 years, distributed sediment models have been coupled with downscaled climatic forecast scenarios and used to assess climate change impacts on soil erosion (e.g. Wilby et al. 1999; Middelkoop et al. 2001). More recently, this technique was also employed for sediment transport evaluation under changing climate in the Mediterranean (e.g. Nunes et al. 2008; Bangash et al. 2013).

Nevertheless, the applicability of distributed sediment models is often constrained. One of the most important limitations to sediment model implementation is data availability for its calibration and validation (Cerdà et al. 2013). Continuous sediment yield measurements are very scarce, especially in Mediterranean basins, and are almost exclusively available for small experimental catchments or plots. For this reason, new sediment datasets are required in order to implement models for catchments that are not monitored for sediment. Given the scarcity of meso- to macro-scale sediment-monitored catchments, new sediment data sources are needed to overcome this issue. A promising opportunity to fill this gap is the development of new modelling techniques in order to exploit proxy and soft data (Blöschl 2001; Seibert and McDonnell 2002) for gaining information with the intention of constraining model calibration.

Many authors have already explored this technique, especially focusing on the sediment volume accumulated in lakes and reservoirs as an indirect validation method for modelling sediment yield at the regional scale (Van Rompaey et al. 2003; Alatorre et al. 2010; Bussi et al. 2013). As streams enter reservoirs, their flow velocity reduces, decreasing the stream sediment transport capacity and causing sedimentation. Due to this phenomenon, part of the sediments transported by the stream may be retained behind the dam, forming a deposit. It is estimated that the annual loss in storage capacity of the world's reservoirs due to sediment deposition is around 0.5–1 % (Verstraeten et al. 2003). For many reservoirs, however, annual storage reduction rates are much higher and can reach 4 or 5 %, such that they lose the majority of their capacity after only 25–30 years (Verstraeten et al. 2003).

Reservoir sediment deposits have been used since the 1950s as an estimate of catchment sediment yield to compare with the results of empirical equations. Nevertheless, this technique was not extensively used until the 1980s (e.g. Jolly 1982; Le Roux and Roos 1982; Duck and McManus 1993). It has been usually employed for determining long-term mean annual sediment yield of large catchments (e.g. Sanz Montero et al. 1996; Verstraeten et al. 2003; Baade et al. 2012). In the past 15 years, lake and reservoir sediment deposits have also been used for distributed model validation (e.g. Srinivasan et al. 1998; de Vente et al. 2005; de Vente et al. 2008; Alatorre et al. 2010; Haregeweyn et al. 2013). All these studies calculated inter-annual soil erosion rates, or sediment yields, averaged over several years. With the above-mentioned models, it is not possible to determine the temporal dynamics of the soil erosion and sediment transport at a smaller temporal scale, such as, for example, the daily scale. A daily model is required in order to evaluate eventual changes in rainfall amount and intensity and their effects on soil erosion in the framework of a climate change study (Mullan et al. 2012). Some attempt to calibrate and validate daily models with reservoir sedimentation volumes has been

carried out in the last years. For example, Raclot and Albergel (2006) applied a distributed model to a catchment in Tunisia and calibrated it by using siltation volumes of a small reservoir. Nevertheless, their results were disappointing concerning reproduction of the sediment transport rates.

In this paper, a distributed hydrological and sediment model, TETIS (Francés et al. 2007; Bussi et al. 2013; Bussi et al. 2014), is used to assess the direct impact of climate change on a highly erodible Mediterranean catchment (the Ésera River catchment, central southern Pyrenees, Spain). The Ésera River drains into the Barasona reservoir, threatening its capacity because of the huge amount of fine sediments that come into it; these sediment deposits are used to calibrate and validate the TETIS sediment sub-model. The suspended sediment series measured by López-Tarazón et al. (2009) at the main tributary of the Ésera (i.e. the Isábena River) are used to check the model reliability. TETIS is subsequently fed with precipitation and temperature scenarios computed with the ARPEGE Regional Circulation Model (RCM) in order to obtain soil erosion and sediment yield scenarios under different climatic conditions. The aim of this study is to implement a daily sediment model at the catchment scale with the absence of gauged sediment data and to assess climate change impact on soil erosion and sediment transport.

2 Case study

The Ésera River catchment is located in the southern central Pyrenees (Spain) and covers 1,532 km² (Fig. 1). The river catchment drains into the Barasona reservoir (ca. 92.2 Hm³). A few kilometres downstream of the reservoir, the Ésera River flows into the Cinca River, one of the main tributaries of the Ebro River. Steep slopes and high altitudes, with several summits surpassing 3,000 m above sea level (a.s.l.), characterise the Ésera River headwaters. At Graus (889.5-km² catchment, Fig. 1), the portions of the catchment above 2,500 and 2,000 m a.s.l. are 9.5 and 27.6 %, respectively. The main tributary of the Ésera River is the Isábena River. It represents almost the 30 % (425.9 km²) of the whole Ésera catchment. It reaches the Ésera River from the left side, a few kilometres upstream of the Barasona reservoir.

The Ésera River catchment, despite being located between two climatic zones (i.e. Oceanic and Mediterranean domains), belongs to the Mediterranean climate, with a high thermal contrast, dry winters with high insulation and stormy summers with torrential precipitations. The land use of the Ésera River catchment is dominated by forest (34 % of all catchment), mainly in the headwaters, with some shrublands (27 %), grassland and pastures (12 %) and arable dry land (10 %) in the lowlands. The rest is mainly composed of alternating urban and arable land. The Ésera River catchment underwent strong land use changes from the mid-twentieth century, mainly due to transformation of cultivated fields into dense

shrub and forest (Beguería et al. 2003; López-Vicente et al. 2008). This was mainly caused by socio-economic reasons which led to cultivated land abandonment, rather than for climatological variations; given that the present study tries to estimate the direct impact of climate change, no land use change was considered for the future scenarios.

The geology of the area is complex and organised in structures from WNW to ESE. The main types of lithology are limestone and shale in the headwaters, limestone and sandstone in the intermediate part, with an important marl strip shaping badland reliefs and producing high amounts of suspended sediment (López-Tarazón et al. 2012) that crosses the whole catchment from west to east close to the middle. Finally, conglomerates and sandstone dominate in the lower part of the catchment.

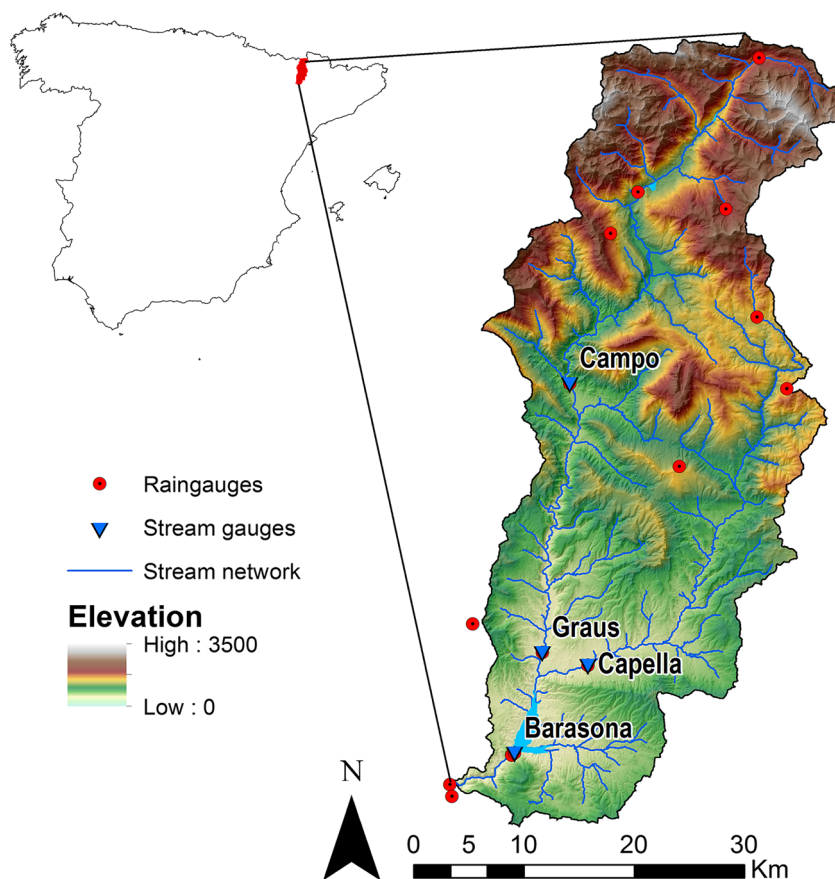
The TETIS model parameters were estimated based on a 100×100-m mesh. A digital elevation model (DEM) and all the DEM-derived parameters were obtained from the National Plan of Aerophotogrammetry (PNOA). Soil parameters were estimated from the European Soil Database (ESDB2 2004). The attributes AWC_TOP (topsoil available water content), ROO (obstacle to roots development depth) and TXT-SRF-DOM (topsoil texture) were reclassified in order to estimate soil capillary retention and infiltration capacity. Percolation capacity was obtained from the lithological map of Spain 1:200,000 (IGME 1994). Land use and vegetation cover were obtained from CORINE 2006 (European Environment Agency 2007), and the C and K USLE factors were obtained from previous studies (e.g. Alatorre et al. 2010).

The Ésera catchment is monitored by several public institutions: the Spanish Meteorological Agency (AEMET) measures daily precipitation and temperature at 12 stations; the Ebro River Water Authority measures 15-min precipitation at 11 rain gauges, temperature at six thermometers and discharge at three stream gauges (Campo, Capella and Graus); while the CEH-CEDEX (National Center for Hydrological Studies) compiles daily water level, volume and outlet discharge of the Barasona reservoir and daily discharges at Campo, Capella and Graus. Moreover, using the already established monitoring network, AEMET developed a new rainfall and temperature-gridded database on a 20×20-km mesh, which covers the whole Spanish peninsular territory (i.e. Spain02; Herrera et al. 2010). In this study, we employed the gridded precipitation and temperature from Spain02, which proved to better describe the orographic effect on the precipitation, as well as the CEH-CEDEX discharge series for calibration and validation of the hydrological sub-model.

Two different sets of sediment information were exploited for model implementation: Barasona reservoir bathymetries and the suspended sediment records measured at the Capella gauging station (Isábena River, main tributary of the Ésera River; López-Tarazón et al. 2009, 2012). The Barasona reservoir depositional history is discussed later.

Suspended sediment transport has been continuously monitored since 2005 by the Fluvial Dynamics Research Group

Fig. 1 Location and general features of the Ésera River catchment, central southern Pyrenees, Spain



(RIUS) at the Capella gauging station. Monitoring is based on automatic and manual water and sediment sampling, together with 15-min turbidity measurements that are later transformed into suspended sediment concentrations (López-Tarazón et al. 2009). Suspended sediment dynamics show that the sediment transport is strongly dominated by extreme events, but base flow also transports a remarkable amount of sediment. Suspended sediment concentrations at Capella are highly variable (varying up to 5 orders of magnitude for a certain discharge) and can be $>300 \text{ g l}^{-1}$ (López-Tarazón et al. 2009).

Mean suspended sediment yield for the 2005–2010 period was $600 \text{ t km}^{-2} \text{ year}^{-1}$. It is known that the suspended sediment texture for the Isábena is rather fine, with an almost total absence of coarse material (i.e. sand). This finding is confirmed by the Barasona bathymetry carried out in 1986, in which only 5 % of sand was found. Given that the coarse material is almost totally trapped in the reservoirs, sandy sediments are not frequent in the Ésera River catchment, and for this reason, we can reasonably assume that suspended sediment transport represents a great portion of the total load. As stated by Webb et al. (1995) and Walling and Fang (2003), suspended sediment measurements are reliable if they account for around the 90 % of the total load, as we assume is the case of the Ésera and Isábena Rivers.

3 Methodology

3.1 The climatological models

The climatic scenarios employed in this study were taken from the PRUDENCE project (Prediction of Regional scenarios and Uncertainties for Defining European Climate change risks and Effects - Christensen et al. 2007). The main goal of the PRUDENCE project was to compute high-resolution climate change scenarios for Europe by means of dynamical downscaling (regional climate modelling) of global climate simulations. This project was carried out by several European research centres, which coupled different Global Circulation Models (GCMs) and RCMs in order to obtain different outputs describing two possible future scenarios selected from the Special Report on Emissions Scenarios (SRES; Nakicenovic and Swart 2000). The A2 and B2 scenarios were selected. These two scenarios are characterised by regionalisation of economic development, with A2 being a more regionally oriented scenario and B2 a more locally oriented scenario.

In this study, we selected and employed the climatic scenarios developed by the French National Centre for Meteorological Research (CNRM). The CNRM coupled the HadAM3 GCM (Cusack et al. 1998) with the ARPEGE RCM (Déqué et al. 1994) and obtained daily series of several

atmospheric variables including precipitation and temperature. HadAM3 is a version of the UK Meteorological Office's United Model. It is a hydrostatic, primitive-equation model with a hybrid vertical coordinate system. In this version of the model, the main model variables are held on 19 levels in the vertical with the lowest level at about 25 m above the surface and the top level at 4.6 hPa (Pope et al. 2000). ARPEGE is a regional circulation model. Its climate version (ARPEGE-Climate) was developed in the 1990s (Déqué et al. 1994). It uses the physical parameterization package of the Metéo-France operational model, with some additions such as the treatment of the ozone concentration as a three-dimensional prognostic variable, a high vertical resolution in the stratosphere (20 levels out of the 30 are above 200 hPa) and a soil-vegetation scheme with rainfall interception. As with all climatic models, these models provide biased daily precipitation and temperature fields, primarily due to model errors and the coarse spatial scale. It is therefore necessary to correct this deviation, as done in various studies (Déqué 2007). In the case of the Ésera River catchment, the correction was carried out by adjusting the quantile plot (or $q-q$ plot) of observed versus simulated daily precipitation and temperature, as demonstrated in the precipitation correction section below.

Climatological scenarios were downloaded from the AEMET website. They consist in daily precipitation and temperature maps for three climatic conditions: control period (1961–1990); A2 scenario (2071–2100); and B2 scenario (2071–2100), with a resolution of 50×50 km. After implementing TETIS in the Ésera River catchment, the model was used to obtain climate-altered series of several hydrological and sedimentological variables. This was done by feeding the TETIS model with precipitation and temperature scenarios computed by means of the ARPEGE model.

3.2 Reconstruction of the depositional history of the Barasona reservoir

Prior to the sediment sub-model calibration and validation, the depositional history of the Barasona reservoir was reconstructed. The historical reconstruction of Barasona storage variations is a complex task because of the high uncertainty of bathymetry values and because there is no comprehensive record of sediment flushing (bottom outlet opening for removing sediment) and dredging (direct extraction of the deposited sediment after emptying the reservoir) operations carried out during the reservoir life.

The reservoir was built in 1932, with a capacity of 71 Hm^3 . In 1971, its capacity was 70.9 Hm^3 and the following year the reservoir was expanded to 92.19 Hm^3 (Valero-Garcés et al. 1999). A bathymetry was carried out in February 1986. The storage value was 91.761 Hm^3 . During this bathymetry, the dry bulk density of the bottom deposits was measured at

1.112 t m^{-3} . The next bathymetry was carried out in December 1993 and provided a storage capacity of 75.940 Hm^3 . In the years 1995, 1996 and 1997, three flushing operations were carried out. These operations are very well documented from an ecological point of view (Avendaño Salas and Cobo Rayán 1998), but the sediment volume extracted was not well quantified. In February 1998, another bathymetry was carried out, in which the capacity was estimated at 84.798 Hm^3 . Following the bathymetry carried out in 1998, the mean sediment texture in the Barasona reservoir is clayey silt (65.87 % silt, 26.56 % clay and 5.57 % sand). Close to the dam body, the clay content increases up to 39.24 %, with the silt and sand content being 60.48 and 0.28 %, respectively. Information about these bathymetries can be found in Mamede (2008). Two bathymetries were also carried out in 2006 and 2007 by the University of Lleida (Spain) within the framework of the Sediment Export from Semi-Arid Catchments (SESAM) project. These results are contained in the project final report (Müller and Francke 2008). The measured storage capacity was 75.78 Hm^3 in June 2006 and 75.18 Hm^3 in May 2007. The period ranging from the construction to February 1998 was not taken into account for sediment sub-model calibration and validation, given that various flushing and dredging operations were carried out and the extracted volumes are unknown. Moreover, significant land use change took place during the 1970s and 1980s, as stated before, making that period unsuitable for model calibration.

3.3 The hydrological and sedimentological model

The TETIS model is a conceptual distributed hydrological and sediment model developed by the Technical University of Valencia (Spain). The TETIS hydrological sub-model has been applied to a wide variety of catchments (e.g. Andrés-Doménech et al. 2010; Salazar et al. 2013; Cowpertwait et al. 2013). It is a grid-based model, which takes advantage of all the spatially distributed information available. It is based on a tank structure, i.e. all hydrologically relevant processes are described by means of a tank balance and simple linear reservoir and threshold equations with physically based parameters. TETIS takes into account precipitation, snow melting, vegetation interception, soil capillary retention, soil infiltration, direct runoff generation, interflow, aquifer storage, base flow and water losses. The grid cells are classified into hillslope, gully and river channel cells, depending on their drainage area. The channel routing is carried out by using the geomorphologic kinematic wave (Francés et al. 2007). The calibration of the TETIS hydrological sub-model is carried out by adjusting up to nine correction factors which multiply nine parameter maps, preserving the spatial structure of the parameters (Francés et al. 2007). An automatic calibration tool is available for model calibration.

The Ésera River catchment hydrological sub-model was calibrated at the Capella gauging station with a daily time step. This time step was chosen in order to reproduce the high temporal variability of the Ésera River catchment sediment transport—also observed by López-Tarazón et al. (2009) in the Isábena—and which will be impossible to analyse by modelling with a monthly or annual time step.

The TETIS sediment sub-model (Bussi et al. 2013; Bussi et al. 2014) is based on the conceptualisation of the CASC2D-SED model (Johnson et al. 2000). The sediment transport depends on the balance between sediment availability and the sediment transport capacity of the stream (Julien 1995). Sediment production on hill slopes is calculated by means of the modified Kilinc and Richardson equation (Kilinc and Richardson 1973; Julien 1995). In-channel transport capacity is given by the Engelund and Hansen equation (Engelund and Hansen 1967). These two formulae are used to route all available sediments towards the downstream cell. Suspended sediments are firstly routed downstream; then, if there is residual capacity, previously deposited sediments are also transported. Lastly, using the residual transport capacity, the parental material is also routed towards the downstream cell. Depending on the settling velocity of each grain size class, the downstream cell material is divided into deposited and suspended material.

The TETIS sediment sub-model was calibrated and validated for the Barasona reservoir by adjusting both transport capacities (hillslope and channel) in order to reproduce the reservoir depositional history. The dry bulk density of the deposited sediment was computed by means of the Miller (1953) formula, which takes into account the temporal variability of dry bulk density, with Lane and Koelzer (1943) coefficients for submerged sediments. Simulated texture was used as input of Miller formulae. In order to take into account the temporal variability of dry bulk density, its temporal evolution was computed. This was done by assigning an initial density value corresponding to unconsolidated conditions to the sediment layer deposited during a given hydrological year (using the Miller formula) and increasing this value year by year (also using Miller formula, which takes into account the age of the deposit). The resulting mean dry bulk density was the weighted mean of all deposited layers. It is expected that older layers will have a higher dry bulk density due to consolidation processes. The sediment trap efficiency was estimated by using the Brune (1953) curves. Given that the reservoir storage capacity varies (between 70 and 92.2 Hm³, based on the available literature), as well as the mean annual inflow, consequently the sediment trap efficiency will also vary during the simulation period. The mean annual inflow is ~400 Hm³ year⁻¹ for the period 1988–1998 and ~500 Hm³ year⁻¹ for the period 1998–2007. These two values were used to take into account the variation of the mean annual inflow for trap efficiency estimation. Following Brune's curves, the expected trap efficiency should be

between 80 and 90 %. This value agrees with Avendaño Salas et al. (1997) and Alatorre et al. (2010), who calculated the trap efficiency as 86 and 90 %, respectively.

4 Results and discussion

4.1 Model implementation

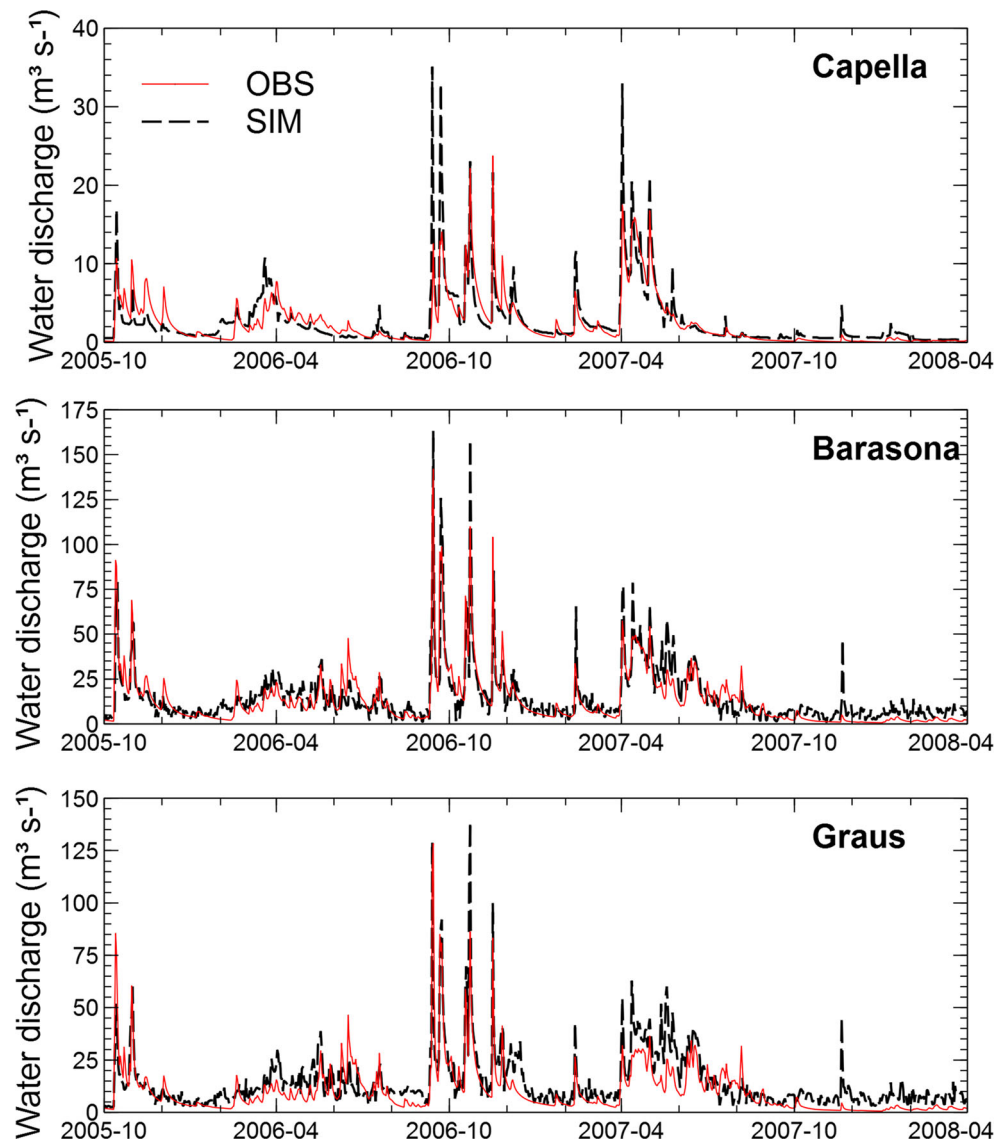
4.1.1 Hydrological modelling

The selected calibration period for the hydrological sub-model was from January 1, 2005 (date/month/year) to January 10, 2008 and the validation period from January 10, 1997 to January 10, 2005. The hydrological sub-model was also spatially validated at the Graus and Campo stream gauges and against the observed discharge entering the Barasona reservoir. The results can be seen in Fig. 2 and Table 1. In general, the model performances are between good and very good, following the classification of Moriasi et al. (2007), both in calibration and in validation. It is important to underline that the peak flow reproduction is satisfactory in all stations. The performance at the Campo gauging station is not as good as at the other stations, although the peak flow reproduction is also correct. This is because the base flow is not properly simulated, probably due to a bad reproduction of the aquifer dynamics and the presence of a small dam for hydropower production. However, given that the aim of this study is the reproduction of the sediment cycle, the focus was put on high flows, since we assume that they are responsible for most of the sediment transport. For this reason, the Ésera River catchment hydrological sub-model can be considered satisfactorily calibrated. The hydrological sub-model results evidence the existence of a fluctuating but constant base flow, which increases during the periods of snow melting, alternated by high peaks mainly composed of direct runoff, which are especially concentrated in autumn and spring.

4.1.2 Sedimentological modelling

Following the bathymetrical history of the Barasona reservoir (Table 2), the sediment sub-model was calibrated by adjusting the sediment sub-model correction factors for reproducing the 1998–2006 sediment accumulation in the Barasona reservoir. This time period was selected because it is considered as most representative of the total series and because the hydrological sub-model calibration was also carried out in part of that period (2005–2007). The model was then validated in the period 2006–2007. The model results (Table 2 and Fig. 3) can be considered satisfactory, taking into account the high uncertainty lying behind the calibration data. As can be seen in Fig. 3, the most relevant reservoir storage losses correspond to

Fig. 2 Hydrological sub-model calibration and spatial validation results (hydrographs). *OBS* observed, *SIM* simulated



the highest water discharge peaks, although the relationship is not directly proportional, due mainly to the rainfall spatial variability and to the antecedent conditions of deposited sediment in the stream network.

Table 1 Hydrological sub-model calibration and spatio-temporal validation results for the study river basins, central southern Pyrenees, Spain

Station	Calibration period		Validation period	
	NSE	VE%	NSE	VE%
Capella	0.720	-6	0.686	-39
Graus	0.581	-28	0.704	-61
Campo	0.294	-44	0.455	-35
Barasona	0.708	-10	0.529	-22

NSE Nash-Sutcliffe efficiency index, *VE* volume error)

The simulated sediment texture is 5 % sand, 50 % silt and 45 % clay. Comparing this result with the measured texture of the deposited sediment inside the reservoir (measured during the bathymetry carried out in 1986), it can be observed that the model obtained a very good approximation, although the simulated sediment is slightly more clayey. This is because the reservoir trap efficiency was not computed for each textural class, given that the trap efficiency calculated by the Brune curves does not depend on the sediment texture. Coarse sediment is generally trapped more easily than finer material in reservoirs, and we suppose that is why simulated texture is slightly finer than the observed one.

Concerning the dry bulk density, results show that, although the variation of the mean deposit density is small (range=1.03–1.04 t m⁻³), the general trend is towards consolidation of the deposit with an increase in the bulk density. This was only contrasted by the highest sediment loads, brought by

Table 2 The observed and simulated deposited sediment volumes for the Barasona reservoir

Period	Accumulated sediments, Hm ³	Specific sediment yield, Mg ha year ⁻¹	Simulated volume, Hm ³
1998–2006	9.02	8.2	9.02
2006–2007	0.60	4.35	0.76

the most extreme events, which makes the dry bulk density decrease. The mean value is close to the measured value of 1.112 t m^{-3} . The difference can be due to consolidation processes that took place during the drawdown periods which the Miller formula does not take into account. Concerning the computed trap efficiency, the range of values obtained by the methodology explained above spans from 0.82 to 0.84.

In order to properly validate the Ésera River catchment model, suspended sediment data measured at the Capella gauging station (Isábena River) were used. These data records only quantify the suspended sediment transport, while the TETIS model uses a total load equation (Engelund and Hansen equation) that estimates both suspended sediment and bed load. Therefore, the two quantities are not directly comparable. However, the comparison between the series can provide interesting conclusions, such as the order of magnitude of the transport processes. Moreover, as stated before, the suspended sediment of the Isábena River represents the most important part of the total transport. The results can be seen in Fig. 4.

It can be noticed that TETIS model results tend to overestimate observed sediment discharge, which is consistent with the comments stated above. In order to carry out a more detailed analysis, the Capella series was separated into three relevant periods: a first period with medium intensity events (maximum simulated discharge= $0.4 \text{ m}^3 \text{ s}^{-1}$; Fig. 4b); a

second high intensity period (maximum simulated discharge= $1.5 \text{ m}^3 \text{ s}^{-1}$; Fig. 4c); and a third low intensity period (maximum simulated discharge= $0.08 \text{ m}^3 \text{ s}^{-1}$; Fig. 4d). Analysing these graphs (Fig. 4b–d), it can be concluded that, in the majority of the cases, the model is forecasting sediment mobilisation, i.e. whether sediment transport takes place or not. The model reproduces adequately the low intensity events but overestimates the high intensity ones. The observed, but not simulated, peaks in Fig. 4c, d correspond to rainfall events not properly simulated by the hydrological sub-model. In fact, the simulated water discharge of those events underestimates the observed discharge, mainly due to the observed rainfall, which probably underestimates the actual rainfall. For example, for the non-simulated event depicted in Fig. 4c (September 19, 2006), the observed discharge was $33 \text{ m}^3 \text{ s}^{-1}$, while the simulated discharge was $14 \text{ m}^3 \text{ s}^{-1}$. Concerning the overestimated peaks of Fig. 4b, the problem is the opposite: the hydrological sub-model overestimates the peaks of October 10, 2005 and October 30, 2005 (second and third peak in Fig. 4b), also due to rainfall overestimation.

The non-linearity of sediment transport enhances the errors of the hydrological sub-model and enlarges the difference between observed and simulated sediment transport. Nonetheless, the behaviour of both the hydrological and sedimentological sub-models can be considered satisfactory, given the spatial and temporal validation results and taking into account the errors in the input data (precipitation, water discharge and sediment discharge) and in the model parameter estimation.

Concerning the November 16, 2006 event (the huge peak in Fig. 4c), given that the hydrological sub-model behaves correctly in this case, the sediment error is not due to hydrological model errors. A first explanation may be that the most severe events, such as those in August 2005 and September 2006, mobilise a great quantity of bed load, which was not

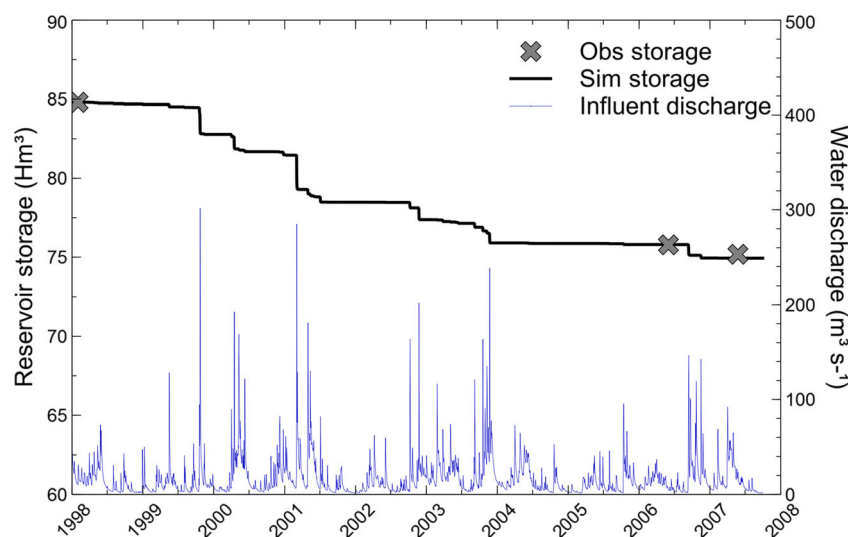
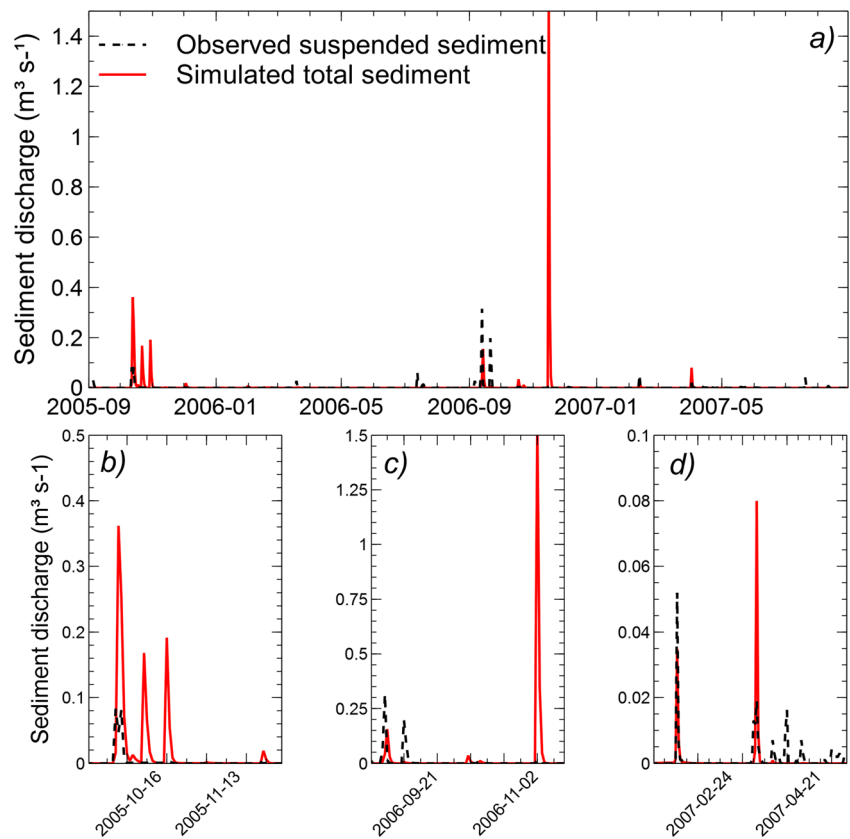
Fig. 3 The evolution of the storage capacity and observed daily inflow of the Barasona reservoir

Fig. 4 a–d TETIS sediment sub-model validation vs gauged suspended sediment at the Capella station



measured. However, this is not sufficient to explain it entirely, given that the sediment transported by the Isábena River is especially fine. Nevertheless, the model simulates a sand content of $\sim 4\%$, in accordance with reality.

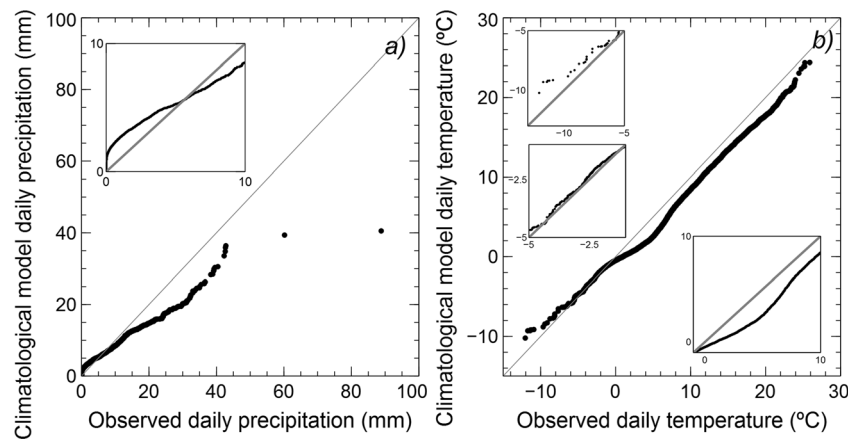
Another possibility relates to the suspended sediment transport measuring methodology. The Capella suspended sediment data series were obtained after conversion of the turbidity register, measured by a high-range backscattering turbidimeter (calibrated with manual and automatic samples), into suspended sediment concentration. Turbidimeter measurements carry a high uncertainty when the fluid concentration is elevated, due to particle size effects on water turbidity (Olive and Rieger 1988). Some authors are also critical with turbidimeter measurements in marly zones with badlands (e.g. Regúés and Nadal-Romero 2013). In particular, these authors, after studying the suspended sediment transport of a micro-scale catchment climatically similar to the Ésera River, stated that a great underestimation of the sediment transport can occur when the transported material is mainly composed of silt and clay and when the concentration overcomes a threshold (e.g. 100 g l^{-1}). The correction factor for adjusting the measured value can be up to 6, due to the fact that the hyper-concentrated flow has a higher transport capacity than still water. The Isábena River fulfils the conditions described by these authors, and, therefore, this is likely to be the main cause of the observed, simulated value difference for high-intensity

events. In this case, the model provides a suspended sediment concentration 2.4 times higher than the observed one.

4.2 Climatological output correction

Climatological outputs (precipitation and temperature) are usually affected by model errors and scale effects and must be corrected in order to reproduce the observed variables. As stated by Déqué (2007), the correction cannot be carried out by comparing each meteorological station with the nearest grid point of the climatological field, but it should be done by comparing areal averaged values. For this reason, mean catchment daily precipitation and temperature series were computed both for observed precipitation and temperature (from $20 \times 20 \text{ km}$ gridded dataset Spain02) and climatological precipitation and temperature (from $50 \times 50 \text{ km}$ gridded ARPEGE model results for control period). Commonly, correction is performed on monthly means (Déqué 2007). However, due to the daily scale of this study, we decided to build precipitation and temperature quantile (or $q-q$) plots, by ranking daily observed and simulated precipitation and observed and simulated temperature (Fig. 5). Both temperature and precipitation are spatially averaged over the Ésera River catchment. In Fig. 5a, it can be noticed that climatological precipitation generally underestimates highest observed precipitation. Nevertheless, it can be observed that from 0 to

Fig. 5 **a, b** Quantile plots of ranked precipitation (*left*) and temperature (*right*). The windows represent zooms of selected parts of the plots



7 mm, climatological precipitation overestimates the observed daily precipitation (Fig. 5, left, in the zoom square located in the upper left corner of the graph). A systematic linear bias can be detected and was corrected by means of a linear regression. The climatological precipitation was then modified by applying a correction equal to the difference between the 1:1 line ($y=x$) and the linear interpolation of precipitation $q-q$ plot (found to be $y=0.73x+0.78$). The equation used to correct precipitation is therefore as follows:

$$P_{sim,corr} = 1.27P_{sim} - 0.78 \tag{1}$$

where $P_{sim,corr}$ is the corrected climatological daily precipitation, and P_{sim} is the original climatological precipitation.

In the same way, the temperature $q-q$ plot (Fig. 5, right) showed an important bias for values >1.5 °C (Fig. 5 right, lower right zoom). Values between -5 and 0 °C correctly reproduced observed temperatures (Fig. 5, right, middle left zoom), and values <-5 ° underestimated them (Fig. 5, right, upper left zoom). For this reason, a different correction was applied depending on the temperature:

$$T_{sim,corr} = T_{sim} + \alpha \tag{2}$$

where $T_{sim,corr}$ is the corrected climatological daily temperature, T_{sim} is the original climatological temperature and α is a correction factor given by:

$$\alpha = 0.4T_{sim} + 2 \quad \text{if } T_{sim} < -5 \text{ } ^\circ\text{C} \tag{3}$$

$$\alpha = 0 \quad \text{if } -5 \text{ } ^\circ\text{C} \leq T_{sim} < -1 \text{ } ^\circ\text{C} \tag{4}$$

$$\alpha = 0.6T_{sim} + 0.6 \quad \text{if } -1 \text{ } ^\circ\text{C} \leq T_{sim} < 1.5 \text{ } ^\circ\text{C} \tag{5}$$

$$\alpha = 1.5 \quad \text{if } T_{sim} \geq 1.5 \text{ } ^\circ\text{C} \tag{6}$$

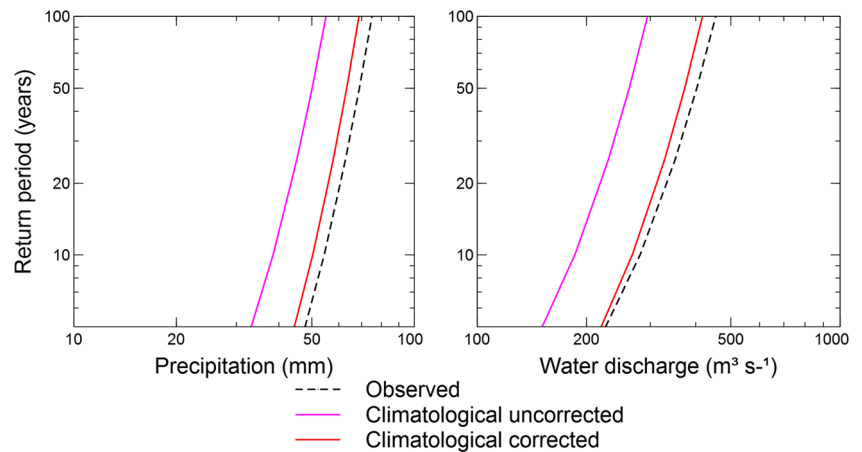
In order to ensure the reliability of corrected climatological variables, the correction must be validated. Since the main goal of this study is to assess climate change impact on sediment yield, the effect of correction should be relevant for extreme rainfall and discharge values. For this reason, the cumulate distribution functions of annual maximum daily precipitation and discharge values were computed and interpolated using a Gumbel distribution function (Fig. 6).

Figure 6 shows that both precipitation and water discharge distribution functions are clearly closer to the observed one after climatological output correction. Water discharge, which is a key variable, shows the best adjustment.

4.3 Climate change assessment

The impact of climate change on the hydrological and sedimentological cycle of the Ésera River catchment was assessed by comparing the results obtained by TETIS for the control scenario (1961–1990) with the ones obtained under A2 and B2 conditions (2070–2100). From Table 3, it can be seen that a general decrease in total precipitation is forecasted for the Ésera River catchment, corresponding to 13 and 12 % of the current mean annual precipitation, respectively, for scenario A2 and B2. A sharp increase in temperature is also observed, with a mean increase of 4.07 °C for A2 scenario and 3.02 °C for B2 scenario. Due to both phenomena, soil moisture content is expected to strongly decrease by 27 and 23 %, respectively. The most abrupt change is represented by the snow-pack, which decreases by 69 and 61 %, respectively. These trends lead to a decrease in water availability. Total water yield is expected to decrease by 40 and 35 %, respectively. Sediment yield shows a surprising behaviour as A2 scenario results indicate a strong decrease by ~50 %, while B2 scenario results point out a small increase of 10 %. The decreasing trend is in contrast with what was obtained in similar recent

Fig. 6 Gumbel distribution function of annual maximum daily precipitation (*left*) and water discharge (*right*), for observed, uncorrected and corrected climatological values



studies (e.g. Coulthard et al. 2012; Mouri et al. 2013), although those applications were developed in different climatic areas. This phenomenon cannot be explained by a simple analysis of global mean values. In order to explain this singularity and assess climate change impact more in detail, monthly means and extreme values of all variables were also analysed.

Figure 7 (left) shows the impact of climate change on precipitation monthly means. An important decrease in the spring peak can be observed. This graph suggests that the precipitation regime is shifting from a bimodal regime with a predominance of spring rainfalls towards a bimodal distribution with a predominance of autumn rainfall or even a unimodal regime. Figure 7 (right) show the distribution functions interpolated with a Gumbel function of annual maximum daily precipitation. This plot describes the climate change impact on extreme events. As can be observed, extreme precipitation values are expected to increase, in spite of the global rainfall decrease observed in Table 3. This phenomenon has already been documented in various papers (e.g. Alpert et al. 2002). Extreme precipitation is expected to increase more under B2 scenario than under A2 scenario. This aspect is likely to affect soil erosion and sediment yield.

Figure 8 shows the monthly means of soil saturation and mean catchment snow depth. The effect of climate change is clear; soil saturation during summer is expected to strongly

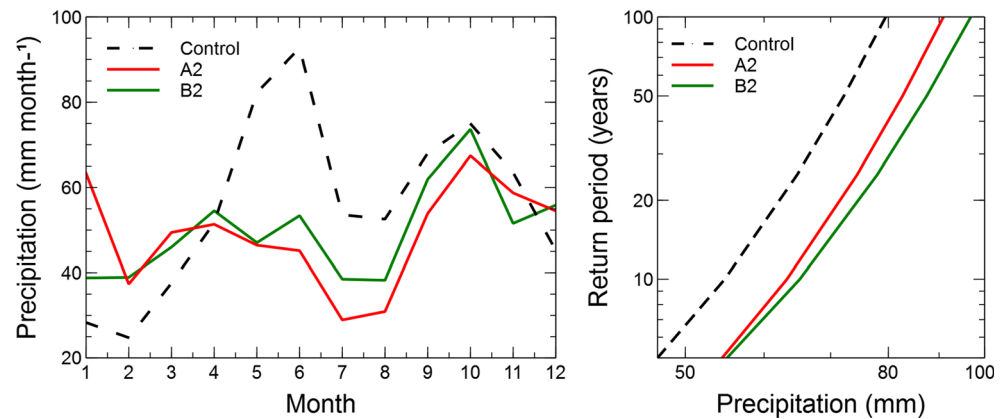
decrease due to precipitation decrease, while snow depth is expected to decrease during winter–spring, due to the increase in mean temperature. Specifically, permanent snow is expected to disappear in summer, as already stated by other authors (e.g. López-Moreno et al. 2009).

Figure 9 (left) shows the monthly mean water discharge. Due to reductions in precipitation and soil saturation, water availability is expected to decrease especially in summer, while in winter, the mean water availability seems to be similar to the control period, probably due to an early snow melting and to an increase in winter precipitation (Fig. 7, left). Figure 9 (left) shows the distribution functions interpolated with a Gumbel function of annual maximum daily water discharge. Surprisingly, extreme water discharge values are expected to decrease in spite of the extreme precipitation increase. Annual maximum water discharge values are expected to decrease under A2 scenario, while under B2 scenario, the difference with the control scenario is small. This is due to a combination of all the effects described above: decrease in total rainfall, soil moisture content and snow depth, along with an increase in extreme precipitation. Reduction of total precipitation and soil moisture content causes a decrease in water availability, although for extreme flood events, precipitation is expected to increase, leading to a small reduction in large discharge peaks especially under scenario B2. Extreme rainstorms and extreme floods are responsible for a large part of

Table 3 Climate change impact on mean values of the main hydrological and sedimentological inputs and state variables for the control and two scenarios (see text for details)

Mean state variable	Control scenario	A2 scenario	B2 scenario	A2 variation	B2 variation
Precipitation (mm year ⁻¹)	686	596	607	-13 %	-12 %
Temperature (°C)	7.99	12.06	11.01	4.07 °C	3.02 °C
Soil moisture (%)	74	54	57	-27 %	-23 %
Snowpack (mm)	49	15	19	-69 %	-61 %
Water yield (Hm ³ year ⁻¹)	690.6	417.6	445.8	-40 %	-35 %
Specific sediment yield (Mg ha ⁻¹ year ⁻¹)	6.33	3.62	7.04	-43 %	11 %

Fig. 7 Climate change impact on monthly mean precipitation (*left*) and annual maximum daily precipitation (*right*)



the landscape evolution in Mediterranean areas and very often transport several tons of sediment. An example of the geomorphological effect caused by an extreme flood in the Pyrenean area is presented by Serrano-Muela et al. (2013).

Figure 10 (left) represents monthly mean variation in sediment yield. A global decrease under A2 scenario can be seen, although the trend is not so clear for B2 scenario results. In this second case, while the spring peak seems to descend, the autumn peak appears to increase. This apparently strange behaviour denotes a lack of seasonal pattern for sediment yield. This is due to the extreme sensitivity of sediment transport to a few large events. In this case, under B2 scenario, two very large events take place in the year 2091. These events occur in May and October and are responsible for both peaks of B2 scenario in Fig. 10 (left). This means that no conclusion can be deduced by observing the sediment yield monthly mean plot, apart from observing the strong dependence of sediment yield from single high-magnitude and low-frequency events. In Fig. 10 (right), the distribution functions of the annual maximum daily sediment yield can be observed. As seen in Table 3, sediment yield is expected to decrease under A2 scenario and increase under B2 scenario. This confirms the fundamental role of large events on the total sediment yield.

Given that the frequency and magnitude of large events in Mediterranean catchments are extremely variable, the inter-annual variability of sediment yield was also studied. The annual specific sediment yields were calculated year-by-year (30 values) and are plotted in Fig. 11. The mean sediment yield value obviously coincides with the values exposed in Table 3. Although the B2 mean sediment yield is higher than the control scenario mean value, the medians show a decrease in sediment yield (3.07, 1.69 and 1.78 Mg ha⁻¹ year⁻¹ for control, A2 and B2 scenarios, respectively), while the standard deviation is strongly increasing for B2 scenario and decreasing for A2 scenario (11, 5 and 21 Mg ha⁻¹ year⁻¹, respectively). This means that, although there is a general trend which indicates a decrease in soil erosion and sediment yield, the variability is expected to increase for the B2 scenario, leading to the largest extreme events, while for the A2 scenario, a decrease in variability is expected. Moreover, the largest events (out of the 1.5 interquartile range) can be seen also from Fig. 11 (represented as dots): extreme events are larger for the B2 scenario and smaller for the A2 scenario than for the control scenario.

This conclusion suggests that the largest events may increase their proportional contribution to the total sediment yield, i.e. the ratio between sediment load produced by n -

Fig. 8 Climate change impact on monthly mean soil saturation (*left*) and monthly mean snow-pack (*right*)

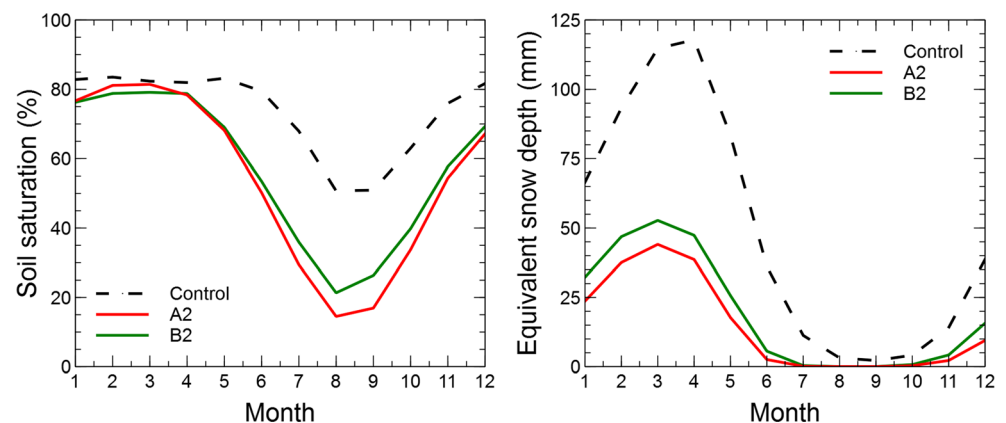
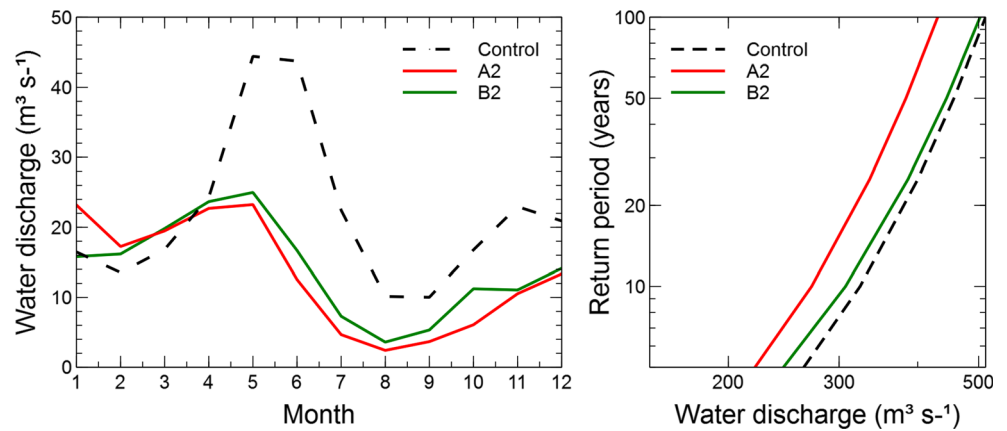


Fig. 9 Climate change impact on monthly mean water discharge (left) and annual maximum daily water discharge (right)



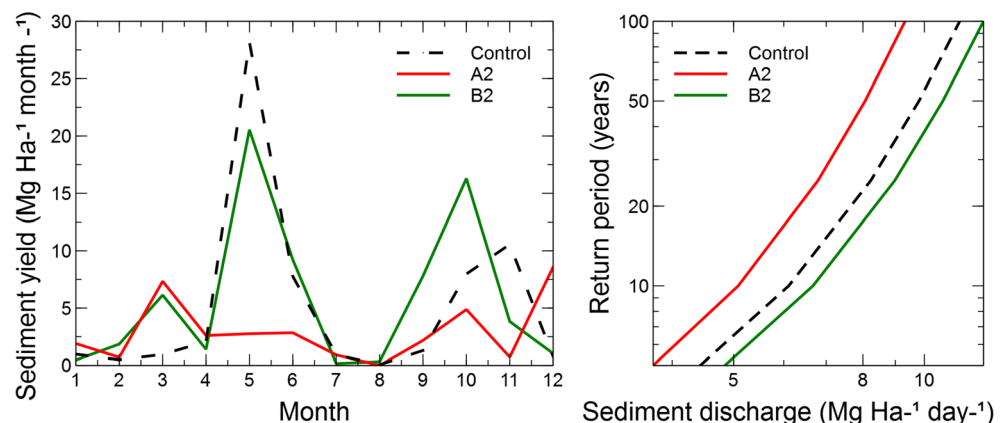
largest events and the total daily events recorded (as explained in González-Hidalgo et al. 2010). For this reason, apart from the magnitude of large events, their relative contribution to total sediment yield must be also taken into account in this study. In fact, the five largest events (in the 30-year series) were responsible of 39.6 36.9 and 49.8 % of total sediment yield for the control, A2 and B2 scenario, respectively. The 10 largest events were responsible of 52.7, 54.8 and 65.1 % of total sediment yield for control, A2 and B2 scenario, respectively, and the 20 largest events were responsible of 62.0, 70.2 and 78.8 % of total sediment yield, respectively. The contribution of the *n*-largest events under the control scenario is similar to what found for other catchments of the same extension by González-Hidalgo et al. (2013), who analysed catchments in North America, while the A2 and B2 scenarios denote a catchment whose sediment cycle is extremely dominated by large events. These values partially agree with Nadal-Romero et al. (2012), who found a similar or higher time compression in a highly erodible small Pyrenean catchment.

This phenomenon can also be seen in Fig. 12, where the relative contribution to total sediment yield of the *n*-largest daily events is represented depending on the number of contributing largest events. It can be noticed that both future

scenarios show a shift towards a more time-compressed sedimentological regime (i.e. more dependent on large events). In the case of the B2 scenario, this means also a small increase in the total sediment yield (Table 3 and Fig. 10, right), while in the case of the A2 scenario, in spite of the increase in relative contribution of the largest daily events, the total sediment yield is expected to decrease.

Therefore, Figs. 10 and 12 suggest that, in the case of the B2 scenario, the decrease in water discharge (both mean and extreme values) is not sufficient to compensate for the shift of the hydrological regime towards a more torrential and vigorous one. This causes an increase in large erosive events and in the total sediment yield. In the case of scenario A2, the increase in rainfall intensity and the shift of hydrological regime towards larger and more relevant flood events are not sufficient to compensate the diminution in global soil moisture and cause a decrease in total sediment yield. However, the increase in time compression is also evident from Fig. 11, owing to the decrease in average sediment yield due to the strong decrease in precipitation and to the lack of large events. Therefore, the most important factors affecting future sediment yields are total precipitation and large daily storm events, as found by Mullan et al. (2012). The expected increase or

Fig. 10 Climate change impact on monthly mean sediment discharge (left) and annual maximum daily sediment discharge (right)



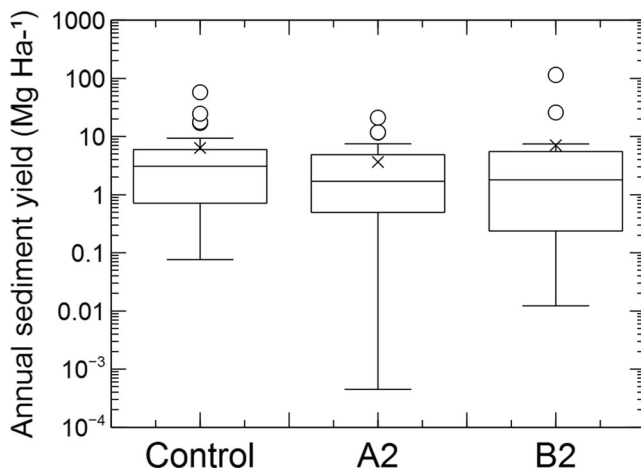


Fig. 11 Boxplot of annual specific sediment yield depending on the climatic scenario (data within the 1.5 interquartile range). Black crosses represent the mean inter-annual specific sediment yield, also presented in Table 3

decrease in sediment yield depends on the occurrence or absence of large events and on the soil moisture of the day of occurrence (i.e. on the storm event timing).

5 Conclusions

This study showed a methodology for implementing a distributed sediment model by exploiting proxy sediment data such as reservoir sedimentation volumes. In situations where reservoir sedimentation data are available, this methodology may help to overcome the problem of lack of sediment erosion and transport information for model calibration and validation. This technique can be applied to a wide range of catchments, given the high number of large reservoirs around the world.

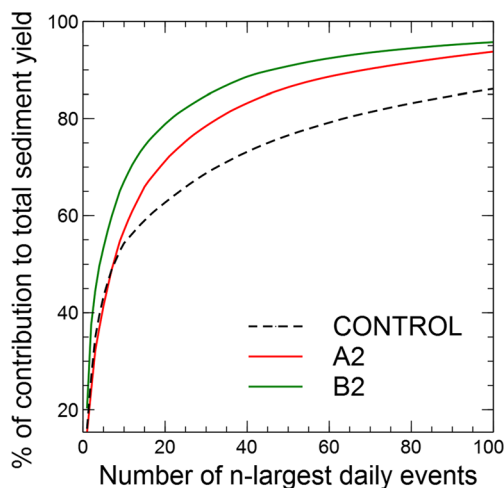


Fig. 12 Percent contribution of the n -largest events (in the 30-year series) to the total sediment yield

Nevertheless, some drawbacks have to be taken into account; for example, the errors in estimation of the sedimentation volume and the availability of a few accumulated sediment volume values (obtained by reservoir bathymetries) for calibrating and validating the model. In order to show this approach, an application of the TETIS model was presented. The model was applied to the highly erodible Ésera River catchment, located in the central southern Pyrenees (Spain), which drains into the Barasona reservoir. The sedimentological history of the Barasona reservoir was reconstructed through a literature analysis and historical bathymetric surveys. Then, the evolution in the reservoir storage capacity was used to calibrate and validate the TETIS sediment sub-model, taking into account the sediment trap efficiency of the reservoir and the dry bulk density of the deposit. The results showed a good performance of the TETIS model, taking into account the high uncertainty affecting all parts of this methodology, such as the deposited sediment volume estimation. The model behaviour was generally satisfactory concerning the material detachment and mobilisation. Furthermore, the model results were verified and analysed by comparing them to the measured suspended sediment discharge at the Capella station. The model acceptably reproduced the small and medium magnitude events, although the error made for high magnitude events was greater. The model results suggest an annual specific sediment yield varying between 0.06 and 68.72 Mg ha⁻¹ year⁻¹. The high inter-annual variability is due to inter-annual changes in the hydrological regime, typical of all Mediterranean-influenced areas.

The model was subsequently employed for analysing the climate change impact on soil erosion and sediment yield, by feeding the model with downscaled climatological scenarios. The results from two future scenarios, called A2 and B2 (2070–2100), were compared with model outputs for the control scenario (1961–1990). In both scenarios, precipitation is expected to decrease, although extreme rainfall events are expected to increase in their magnitude. This effect, along with temperature increments, is expected to cause a general decrease in average soil moisture and especially in the snowpack. The combination of all these result will produce a higher decrease in total runoff resources than it is expected for precipitation. However, concerning floods, the increase of high precipitation will be compensated with the reduction of soil moisture and snowpack, generating smaller floods than at present in both scenarios.

Sediment yield showed a more controversial behaviour, as the A2 scenario indicated a decrease (3.62 Mg ha⁻¹ year⁻¹, -43 %) in average annual specific sediment yield, and the B2 scenario showed an increase (7.04 Mg ha⁻¹ year⁻¹, +11 %). Moreover, the model results showed that the hydrological and sedimentological regime is expected to become more dependent on large events, thus increasing its time compression, under both scenarios.

Acknowledgments This study was funded by the Spanish Ministry of Economy and Competitiveness through the research projects SCARCE-CONSOLIDER (ref. CSD2009-00065) and ECOTETIS (ref. CGL2011-28776-C02-01). Suspended sediment records of the Isábena river and bathymetrical surveys were carried out within the framework of the project “Sediment export from large semi-arid catchments: measurements and modelling (SESAM), funded by the German Science Foundation (Deutsche Forschungsgemeinschaft, DFG). The authors wish to thank the Ebro Water Authorities for permission to install the measuring equipment at the Capella gauging station and for providing hydrological data. Both observed and modelled precipitation and temperature data were provided by the Spanish Meteorological Agency (AEMET). Some of the reservoir bathymetric survey reports were provided by Rafael Cobo Rayán (CEH-CEDEX, National Center for Hydrological Studies).

References

- Alatorre LC, Beguería S, García-Ruiz JM (2010) Regional scale modeling of hillslope sediment delivery: a case study in the Barasona Reservoir watershed (Spain) using WATEM/SEDEM. *J Hydrol* 391:109–123
- Alpert P, Ben-Gai T, Baharad A, Benjamini Y, Yekutieli D, Colacino M, Diodato L, Ramis C, Homar V, Romero R, Michaelides S, Manes A (2002) The paradoxical increase of Mediterranean extreme daily rainfall in spite of decrease in total values. *Geophys Res Lett* 29(11):1536
- Andrés-Doménech I, Múnera JC, Francés F, Marco JB (2010) Coupling urban event-based and catchment continuous modelling for combined sewer overflow river impact assessment. *Hydrol Earth Syst Sci* 14:2057–2072
- Avendaño Salas C, Cobo Rayán R (1998) Seguimiento de los sólidos en suspensión durante el vaciado del embalse de Joaquín Costa. *Limnética* 14:113–120
- Avendaño Salas C, Sanz Montero ME, Cobo Rayán R, Gómez Montaña JL (1997) Sediment yield at Spanish reservoirs and its relationship with the drainage basin area. In: *Proceedings of the 19th Symposium of Large Dams, Florence*. ICOLD (International Committee on Large Dams), pp 863–874
- Baade J, Franz S, Reichel A (2012) Reservoir siltation and sediment yield in the Kruger National Park, South Africa: a first assessment. *Land Degrad Dev* 23:586–600
- Bangash RF, Passuello A, Sanchez-Canales M, Terrado M, López A, Elorza FJ, Ziv G, Acuña V, Schuhmacher M (2013) Ecosystem services in Mediterranean river basin: climate change impact on water provisioning and erosion control. *Sci Total Environ* 458–460C:246–255
- Beguería S, López-Moreno JI, Lorente L, Seeger M, García-Ruiz JM (2003) Assessing the effect of climate oscillations and land-use changes on streamflow in the central Spanish Pyrenees. *Ambio* 32: 283–286
- Blöschl G (2001) Scaling in hydrology. *Hydrol Process* 15:709–711
- Brune GM (1953) Trap efficiency of reservoirs. *Trans AGU* 34:407–418
- Bussi G, Rodríguez-Lloveras X, Francés F, Benito G, Sánchez-Moya Y, Sopena A (2013) Sediment yield model implementation based on check dam infill stratigraphy in a semiarid Mediterranean catchment. *Hydrol Earth Syst Sci* 17:3339–3354
- Bussi G, Francés F, Montoya JJ, Julien PY (2014) Distributed sediment yield modelling: importance of initial sediment conditions. *Environ Model Softw* 58:58–70
- Cerdà A (1998) Effect of climate on surface flow along a climatological gradient in Israel: a field rainfall simulation approach. *J Arid Environ* 38:145–159
- Cerdà A, Brazier R, Nearing M, de Vente J (2013) Scales and erosion. *Catena* 102:1–2
- Christensen JH, Carter TR, Rummukainen M, Amanatidis G (2007) Evaluating the performance and utility of regional climate models: the PRUDENCE project. *Clim Chang* 81(S1):1–6
- Coulthard TJ, Ramirez J, Fowler HJ, Glenis V (2012) Using the UKCP09 probabilistic scenarios to model the amplified impact of climate change on drainage basin sediment yield. *Hydrol Earth Syst Sci* 16:4401–4416
- Cowpervait P, Ocio D, Collazos G, de Cos O, Stocker C (2013) Regionalised spatiotemporal rainfall and temperature models for flood studies in the Basque Country, Spain. *Hydrol Earth Syst Sci* 17:479–494
- Cusack S, Slingo A, Edwards JM, Wild M (1998) The radiative impact of a simple aerosol climatology on the Hadley Centre atmospheric GCM. *Quat J R Meteorol Soc* 124:2517–2526
- De Vente J, Poesen J, Verstraeten G (2005) The application of semi-quantitative methods and reservoir sedimentation rates for the prediction of basin sediment yield in Spain. *J Hydrol* 305:63–86
- De Vente J, Poesen J, Verstraeten G, Van Rompaey A, Govers G (2008) Spatially distributed modelling of soil erosion and sediment yield at regional scales in Spain. *Glob Planet Chang* 60:393–415
- Déqué M (2007) Frequency of precipitation and temperature extremes over France in an anthropogenic scenario: model results and statistical correction according to observed values. *Glob Planet Chang* 57: 16–26
- Déqué M, Dreveton C, Braun A, Cariolle D (1994) The ARPEGE/IFS atmosphere model: a contribution to the French community climate modelling. *Clim Dyn* 10:249–266
- Duck R, McManus J (1993) Sedimentation in natural and artificial impoundments: an indicator of evolving climate land use and dynamic conditions. In: McManus J, Duck R (eds) *Geomorphology and sedimentology of lakes and reservoirs*. Wiley and Sons, Chichester
- Engelund F, Hansen E (1967) A monograph on sediment transport in alluvial streams. Monogr Denmark Tech Univ Hydraul Lab, Teknisk Forlag, Copenhagen
- ESDB2 (2004) The European Soil Database distribution version 2.0. European Commission and the European Soil Bureau Network Office for Official Publications of the European Communities. Luxembourg
- European Environment Agency (2007) CLC2006 technical guidelines EEA technical report no. 17/2007. European Environment Agency, Copenhagen, Denmark
- Francés F, Vélez JJ, Vélez JJ (2007) Split-parameter structure for the automatic calibration of distributed hydrological models. *J Hydrol* 332:226–240
- Foster IDL, Rowntree KM, Boardman J, Mighall TM (2012) Changing sediment yield and sediment dynamics in the Karoo uplands, South Africa; post-European impacts. *Land Degrad Dev* 23:508–522
- González-Hidalgo JC, Batalla RJ, Cerdà A, de Luis M (2010) Contribution of the largest events to suspended sediment transport across the USA. *Land Degrad Dev* 21:83–91
- González-Hidalgo JC, Batalla RJ, Cerdà A (2013) Catchment size and contribution of the largest daily events to suspended sediment load on a continental scale. *Catena* 102:40–45
- Herrera S, Gutiérrez JM, Ancell R, Pons MR, Frías MD, Fernández J (2010) Development and analysis of a 50-year high-resolution daily gridded precipitation dataset over Spain (*Spain02*). *Int J Climatol* 32:74–85
- Haregeweyn N, Poesen J, Verstraeten G, Govers G, de Vente J, Nyssen J, Deckers J, Moeyersons J (2013) Assessing the performance of a spatially distributed soil erosion and sediment delivery model (WATEM/SEDEM) in northern Ethiopia. *Land Degrad Dev* 24: 188–204
- IGME (1994) Mapa geológico de la península ibérica Baleares y Canarias. Instituto Tecnológico Geominero de España, Madrid

- Johnson B, Julien P, Molnar DK, Watson CC (2000) The two-dimensional upland erosion model CASC2D-SED. *J Am Water Resour Assoc* 36:31–42
- Jolly JP (1982) A proposed method for accurately calculating sediment yields from reservoir deposition volumes. In: Proceedings of the Exeter Symposium "Recent developments in the explanation and prediction of erosion and sediment yield". Ed. D. E. Walling. IAHS Publ No 37, IAHS Press, Wallingford, UK
- Julien P (1995) Erosion and sedimentation. Cambridge University Press, Cambridge
- Kilinc M, Richardson EV (1973) Mechanics of soil erosion from overland flow generated by simulated rainfall. Colorado State University Hydrology Papers, Colorado
- Lane EW, Koelzer VA (1943) Density of sediments deposited in reservoirs. Rep No 9 of a Study of Methods Used in Measurement and Analysis of Sediment Loads in Streams, Engineering District, St. Paul, MN, USA, District Sub-Office Univ. of Iowa, USA
- Lavee HA, Imeson C, Sarah P (1998) The impact of climate change on geomorphology and desertification along a Mediterranean-arid transect. *Land Degrad Dev* 9:407–422
- Le Roux JS, Roos ZN (1982) The rate of soil erosion in the Wuras Dam catchment calculated from sediments trapped in the dam. *Z Geomorphol Suppl* 26:315–329
- López-Moreno JI, Goyette S, Beniston M (2009) Impact of climate change on snowpack in the Pyrenees: horizontal spatial variability and vertical gradients. *J Hydrol* 374:384–396
- López-Tarazón JA, Batalla RJ, Vericat D, Francke T (2009) Suspended sediment transport in a highly erodible catchment: the River Isábena (Southern Pyrenees). *Geomorphology* 109:210–221
- López-Tarazón JA, Batalla RJ, Vericat D, Francke T (2012) The sediment budget of a highly dynamic mesoscale catchment: the River Isábena. *Geomorphology* 138:15–28. doi:10.1016/j.geomorph.2011.08.020
- López-Vicente M, Navas A, Machín J (2008) Modelling soil detachment rates in rainfed agrosystems in the south-central Pyrenees. *Agric Water Manag* 95:1079–1089
- Mamede GL (2008) Reservoir sedimentation in dryland catchments: modelling and management. PhD dissertation, University of Potsdam, Universitätsbibliothek
- Middelkoop H, Daamen K, Gellens D, Grabs W, Kwadijk JCI, Lang H, Parmet BWAH, Schädler B, Schulla J, Wilke K (2001) Impact of climate change on hydrological regimes and water resources management in the Rhine Basin. *Clim Chang* 49:105–128
- Miller CR (1953) Determination of the unit weight of sediment for use in sediment volume computations. Bureau of Reclamation Memorandum Denver, Colorado, US
- Milly PCD, Dunne KA, Vecchia AV (2005) Global pattern of trends in streamflow and water availability in a changing climate. *Nature* 438:347–350
- Moriasi DN, Arnold JG, Van Liew MW, Bingner RL, Harne RD, Veith TL (2007) Model evaluation guidelines for systematic quantification of accuracy in watershed simulations. *Trans ASAE* 50:885–900
- Mouri G, Golosov V, Chalov S, Takizawa S, Oguma K, Yoshimura K, Shiiba M, Hori T, Oki T (2013) Assessment of potential suspended sediment yield in Japan in the 21st century with reference to the general circulation model climate change scenarios. *Glob Planet Chang* 102:1–9
- Mullan D, Favis-Mortlock D, Fealy R (2012) Addressing key limitations associated with modelling soil erosion under the impacts of future climate change. *Agric For Meteorol* 156:18–30
- Müller EN, Francke T (2008) SESAM DATA SESAM: sediment export from semi-arid catchments—measurement and modelling (2005–2008). Potsdam, Germany
- Nadal-Romero E, Lasanta T, Gonzalez-Hidalgo JC, de Luis M, García-Ruiz JM (2012) The effect of intense rainstorm events on the suspended sediment response under various land uses: the Aisa valley experimental station. *Cuad Investig Geogr* 38:27–47
- Nakicenovic N, Swart R (2000) Special report on emissions scenarios. Cambridge University Press, Cambridge
- Nearing MA, Pruski FF, O'Neill MR (2004) Expected climate change impacts on soil erosion rates: a review. *J Soil Water Conserv (USA)* 59:43–50
- Nearing MA, Jetten V, Baffaut C, Cerdan O, Couturier A, Hernandez M, Le Bissonnais Y, Nichols MH, Nunes JP, Renschler CS, Souchère V, van Oost K (2005) Modeling response of soil erosion and runoff to changes in precipitation and cover. *Catena* 61:131–154
- Nunes JP, Seixas J, Pacheco NR (2008) Vulnerability of water resources vegetation productivity and soil erosion to climate change in Mediterranean watersheds. *Hydrol Process* 22:3115–3134
- Olive LJ, Rieger WA (1988) An examination of the role of sampling strategies in the study of suspended sediment transport. In *Sediment Budgets*. IAHS Publ 174, IAHS Press, Wallingford, UK, pp 259–267
- Peizhen Z, Molnar P, Downs WR (2001) Increased sedimentation rates and grain sizes 2–4 Myr ago due to the influence of climate change on erosion rates. *Nature* 410:891–897
- Pope VD, Gallani ML, Rowntree PR, Stratton RA (2000) The impact of new physical parametrizations in the Hadley Centre climate model: HadAM3. *Clim Dyn* 16:123–146
- Pruski FF, Nearing MA (2002) Climate-induced changes in erosion during the 21st century for eight US locations. *Water Resour Res* 38:34–1–34–11
- Raclot D, Albergel J (2006) Runoff and water erosion modelling using WEPP on a Mediterranean cultivated catchment. *Phys Chem Earth Parts A/B/C* 31:1038–1047
- Regués D, Nadal-Romero E (2013) Uncertainty in the evaluation of sediment yield from badland areas: suspended sediment transport estimated in the Araguás catchment (central Spanish Pyrenees). *Catena* 106:93–100
- Salazar S, Francés F, Komma J, Blume T, Francke T, Bronstert A, Blöschl G (2013) A comparative analysis of the effectiveness of flood management measures based on the concept of “retaining water in the landscape” in different European hydro-climatic regions. *Nat Hazards Earth Syst Sci* 12(11):3287–3306
- Sanz Montero ME, Cobo Rayán R, Avendaño Salas C, Gómez Montaña JL (1996) Influence of the drainage basin area on the sediment yield to Spanish reservoirs. In: Proceedings of the First European Conference and Trace Exposition on Control Erosion
- Seibert J, McDonnell JJ (2002) On the dialog between experimentalist and modeler in catchment hydrology: use of soft data for multicriteria model calibration. *Water Resour Res* 38(11):23–1–23–14
- Serrano-Muela P, Nadal-Romero E, Lana-Renault N, González-Hidalgo JC, López-Moreno J I, Beguería S, Sanjuan Y, García-Ruiz JM (2013) An exceptional rainfall event in the Central Western Pyrenees: spatial patterns in discharge and impact. *Land Degrad Dev*, Online ver. doi:10.1002/ldr.2221
- Srinivasan R, Ramanarayanan TS, Arnold JG, Bednarz ST (1998) Large area hydrologic modeling and assessment part II: model application. *J Am Water Resour Assoc* 34(1):91–101
- Valero-Garcés BL, Navas A, Machín J, Walling D (1999) Sediment sources and siltation in mountain reservoirs: a case study from the Central Spanish Pyrenees. *Geomorphology* 28:23–41
- Van Rompaey A, Verstraeten G, Van Oost K, Govers G, Poesen J (2001) Modelling mean annual sediment yield using a distributed approach. *Earth Surf Proc Land* 26:1221–1236
- Van Rompaey A, Vieillefont V, Jones RJA, Montanarella L, Verstraeten G, Bazzoffi P, Dostal T, Krasa J, de Vente J,

- Poesen J (2003) Validation of soil erosion estimates at European scale. European Soil Bureau Research Report No13 EUR 20827 EN Office for Official Publications of the European Communities, Luxembourg
- Verstraeten G, Poesen J, de Vente J, Koninckx X (2003) Sediment yield variability in Spain: a quantitative and semiquantitative analysis using reservoir sedimentation rates. *Geomorphology* 50:327–348
- Walling DE, Fang D (2003) Recent trends in the suspended sediment loads of the world's rivers. *Glob Planet Chang* 39:111–126
- Webb BW, Foster IDL, Gurnell A (1995) Hydrology water quality and sediment behaviour. In: Foster IDL, Gurnell A, Webb BW (eds) *Sediment and water quality in river catchments*. Wiley, Chichester, pp 1–30
- Wilby RL, Hay LE, Leavesley GH (1999) A comparison of downscaled and raw GCM output: implications for climate change scenarios in the San Juan River basin Colorado. *J Hydrol* 225:67–91
- Zhao G, Mu X, Wen Z, Wang F, Gao P (2013) Soil erosion, conservation and eco-environment changes in the Loess Plateau of China. *Land Degrad Dev* 24:499–510